Journal of Advanced Research 16 (2019) 35–42

Contents lists available at ScienceDirect

Journal of Advanced Research

journal homepage: www.elsevier.com/locate/jare

Original Article

Tunable surface adsorption and wettability of candle soot coated on ferroelectric ceramics

Gurpreet Singh [1], Moolchand Sharma [1], Rahul Vaish *

School of Engineering, Indian Institute of Technology Mandi, Mandi, Himachal Pradesh 175005, India

HIGHLIGHTS

- Candle soot showed the maximum adsorption of MB dye (~90%) in a basic medium.
- Candle soot-coated BCZTO adsorbed more dye than an uncoated BCZTO sample.
- Candle soot on positively poled side of BCZTO adsorbed more dye in acidic medium.
- Candle soot on negatively poled side of BCZTO adsorbed more dye in basic medium.
- Contact angle of candle soot-coated poled BCZTO changed with the surface potential.

GRAPHICAL ABSTRACT

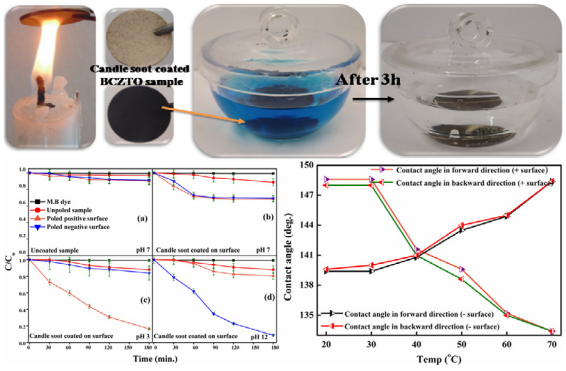

ARTICLE INFO

Article history:
Received 5 October 2018
Revised 1 December 2018
Accepted 18 December 2018
Available online 28 December 2018

Keywords:
Ferroelectric
Hydrophobic
Adsorption
Candle soot
Poling

ABSTRACT

A ferroelectric $Ba_{0.85}Ca_{0.15}Ti_{0.9}Zr_{0.1}O_3$ (BCZTO) ceramic was prepared using a solid-state reaction route. A coating of candle soot was provided on poled and unpoled BCZTO samples. X-ray diffraction and Raman spectroscopy confirmed the presence of the graphite form of carbon in the candle soot. Scanning Kelvin probe microscopy determined that the highest surface potentials were ~34 mV and 1.5 V in the unpoled and poled BCZTO samples, respectively. The candle soot was found to adsorb ~65%, 80%, and 90% of the methylene blue dye present in acidic, neutral, and basic media, respectively, within 3 h. In both the poled and unpoled cases, the BCZTO samples coated with candle soot showed greater adsorption capacities than the uncoated BCZTO sample. In the cases of poled samples coated with candle soot, the adsorption was found to be greater in the case of candle soot coated on a positively charged surface than that for candle soot coated on a negatively charged BCZTO surface in an acidic medium. In a basic medium, the adsorption was found to be greater in the case of candle soot coated on a negatively charged surface than that for candle soot coated on a positively charged BCZTO surface. The contact angle of the candle soot-coated BCZTO sample was found to be hydrophobic (~149°). The contact angle decreased (~149–133°) with an increase in temperature (30–70 °C) in the case of candle soot coated on the positive surface of a poled BCZTO sample. The contact angle increased (~139–149°) with an increase in temperature (30–70 °C) in the case of candle soot coated on the negative surface of a poled BCZTO sample. Internal electric field-assisted (associated with ferroelectric materials) adsorption could be a potential technique to improve adsorption processes.

Introduction

Water pollution is a serious problem faced by many countries all over the world [1,2]. The extensive use of dyes in the textile

Peer review under responsibility of Cairo University.

* Corresponding author.
E-mail address: rahul@iitmandi.ac.in (R. Vaish).
[1] The first two authors contributed equally to this article.

https://doi.org/10.1016/j.jare.2018.12.005
2090-1232/

industries generates coloured wastewater [3,4]. Usually, this wastewater is directly discharged into nearby water sources such as lakes and rivers, which it pollutes [5]. These dyes are very toxic to some aquatic organisms and even cause dermatitis, skin irritation, cancer, and allergies in humans [6,7]. Several techniques have been used to solve water pollution problems, including photocatalysis, adsorption, membrane filtration, ion exchange, and coagulation [8]. Various studies have been reported involving dye degradation and antimicrobial processes through photocatalytic active coatings [9–13]. Amongst these, adsorption through activated carbon is an effective technique for the decolourisation of wastewater [5,14]. The limitation imposed by the high cost of activated carbon has been removed by the use of low-cost alternatives for the adsorption of dyes, such as fly ash, sugar beet pulp, and activated carbon, obtained from fertiliser waste and wood [6]. Similarly, candle soot (carbon derived from candle wax) is another low-cost and easily available adsorbent for the adsorption of dyes. Recently, Singh *et al.* reported the use of candle soot as an adsorbent for the adsorption of two dyes (methylene blue and rhodamine B), and obtained adsorption values of 55% and 95%, respectively, within 2.5 h [15]. Moreover, the hydrophobic/superhydrophobic nature of candle soot coatings on some substrates has been reported [16]. Various hydrophobic/superhydrophobic surfaces, such as meshes, coatings, sponges, and fabrics, have been used in various applications, including oil–water filtration and the adsorption of various oils [17–19]. To benefit from the adsorption and hydrophobic/superhydrophobic characteristics of candle soot, it must be coated on some substrate. In the context of adsorption, electrosorption is another phenomenon in which an external electric field significantly improves the adsorption of organic pollutants. The external field forces the charged species of organic pollutants (dyes) towards the oppositely charged surface, which enhances the adsorption [20,21]. Electrosorption requires an external power source, which will add extra cost. On the other hand, ferroelectric materials have a remnant polarisation, which can support electrosorption. Ferroelectric materials have a wide range of applications such as piezoelectric and pyroelectric energy harvesting [22,23], manufacturing of oscillators [24], filters [25], thermistors [26], photovoltaic cells [27], and photocatalytic degradation of dyes [28]. The internal electric field present in a ferroelectric material prevents the recombination of electron and hole pairs during photocatalysis, and therefore, helps to increase the photocatalytic degradation of organic dye pollutants [29]. In a similar manner, it was interesting to investigate the effect of positive and negative ferroelectric surfaces on the adsorption of organic dye pollutants, which had not previously been explored.

This study investigated the influence of ferroelectricity on the adsorption behaviour of candle soot. In addition, the effect of ferroelectricity on the hydrophobicity of the candle soot coated on a ferroelectric sample was also investigated.

Experimental

A $Ba_{0.85}Ca_{0.15}Ti_{0.9}Zr_{0.1}O_3$ (BCZTO) ceramic was prepared using a solid-state reaction route. $BaCO_3$, CaO, ZrO_2, and TiO_2 powders (Sigma-Aldrich, St Louis, MO, USA) were utilised according to their stoichiometry. These powders were manually mixed in an agate mortar for 1 h. After mixing, the mixture was ball-milled for 4 h in an acetone medium to obtain a homogenous and fine powder. The powder was calcined at 1200 °C for 4 h in a Nabertherm furnace (Nabertherm GmbH, Bahnhofstr, Lilienthal, Germany). A polyvinyl alcohol (PVA) (2 wt%) binder was next added to the calcined powder. Then, the mixture of calcined powder and binder was pressed to form green pellets with a diameter of 24 mm and thickness of 1 mm. These pellets were sintered at 1400 °C for 4 h to form a single phase of BCZTO. The BCZTO sample was characterised using an X-ray diffraction (XRD) technique to confirm the phase formation. A Rigaku diffractometer (Rigaku Corporation, Akishima-shi, Tokyo, Japan) with a 9 kW rotating anode (Cu Kα) was used to obtain the XRD pattern. The samples were scanned in the range of 20–80° with a scanning speed of 2°/min. The candle soot was characterised using XRD and Raman spectroscopy to reveal the forms of carbon present in the candle soot, along with their vibrational modes. The Raman spectrum was obtained using a HORIBA instrument (Model-LabRAM HR Evolution, HORIBA Scientific, Kisshoin, Minami-Ku, Kyoto, Japan). A 532-nm laser was used as an excitation source. The Brunauer–Emmett–Teller (BET) method was used to measure the surface area of candle soot particles using an Autosorb iQ Station 2 (Quantachrome Instruments, USA) with N_2 at 77 K. An electric poling treatment was performed on the BCZTO samples using 3 kV/mm. To obtain the surface potentials of the unpoled and poled BCZTO samples, a scanning Kelvin probe microscopy (SKPM, multimode8, Bruker, USA) technique was used. Samples with an area of $1 \times 1\ \mu m^2$ were scanned at a scanning rate of 0.8 Hz during the SKPM measurements. The unpoled and poled samples were given a candle soot coating by directly exposing their surfaces to a candle.

The surface morphologies of the coated and uncoated BCZTO samples were observed using field emission scanning electron microscopy (FE-SEM). In the adsorption experiment, methylene blue (MB) dye was used as the adsorbate, which is one of the commonly found pollutants in wastewater [30]. The chemical formula of MB dye is $C_{16}H_{18}ClN_3S{\cdot}3H_2O$ [31]. The MB dye adsorption study was performed using candle soot, a candle soot-coated unpoled sample, a poled sample with candle soot on the positive surface, and a poled sample with candle soot on the negative surface. For the adsorption experiments, quartz cuvettes were filled with 10 mL of the MB dye solution. Each sample was dipped into a quartz cuvette containing the dye solution. A quartz cuvette was placed in the dark to perform the adsorption experiment. In the case of a poled sample, the coated side was exposed to the dye solution, and the uncoated side was covered with cellophane tape. Test samples (1 mL) were collected every 30 min. A UV–visible spectrophotometer (SHIMADZU- UV 2600, SHIMADZU company, Chiyoda-ku, Tokyo, Japan) was used to measure the unknown dye concentrations in the test samples. The contact angles of the candle soot-coated poled and unpoled BCZTO samples were measured using a contact angle apparatus (SEO, Phoenix 300, Seoul, South Korea) to investigate the effect of ferroelectricity on the contact angle.

Results and discussion

Fig. 1 shows the typical process for the deposition of candle soot on the BCZTO sample. This figure also shows the typical adsorption behaviour of the candle soot-coated BCZTO sample.

Fig. 2(a) shows the XRD pattern obtained for the uncoated BCZTO sample. Various sharp peaks are observed at angles of 22.26°, 31.64°, 38.88°, 44.85°, 51.1°, 56.25°, 66.12°, 70.35°, 75.09°, and 79.47°. These peaks exactly match the references for BCZTO [32,33]. It shows the formation of a single phase of BCZTO in the sample, with no impurity phase. The peaks observed at 22.26°, 31.64°, 38.88°, 44.85°, 51.1°, 56.25°, 66.12°, 70.35°, 75.09°, and 79.47°correspond to the (1 0 0), (1 1 0), (1 1 1), (0 0 2), (2 0 0), (2 1 1), (2 2 0), (2 2 1), (3 1 0), and (3 1 1) atomic planes, respectively. Fig. 2(b) shows the XRD pattern obtained for the candle soot. Two peaks are observed in the XRD pattern. One high-intensity broad peak is observed at 24.98°, and another low-intensity broad peak is observed at 42.96°. Usually, broad peaks indicate an amorphous or nano-crystalline nature. Based

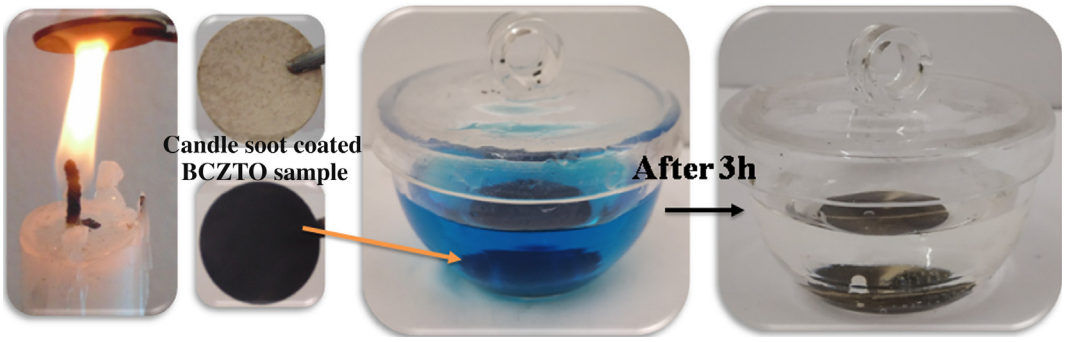

Fig. 1. Candle soot coating process along with adsorption experiment.

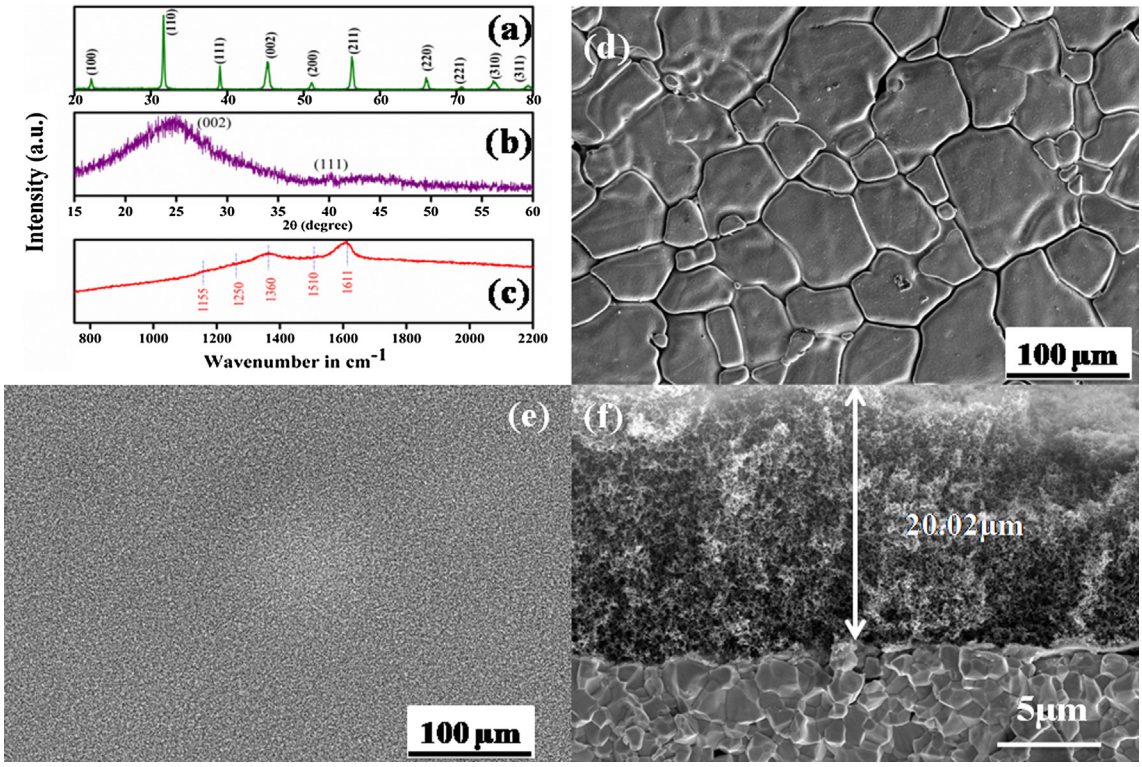

Fig. 2. (a) XRD pattern of uncoated BCZTO sample; (b) XRD pattern of candle soot powder; (c) Raman spectrum of candle soot powder; (d and e) SEM micrographs of uncoated and coated BCZTO samples, respectively; and (f) SEM micrograph of cross-section of coated BCZTO sample.

on the literature available on the various structural possibilities for the carbon present in candle soot, which include graphite, diamond, and carbon-nanotubes, these peaks are a good match for graphite (hexagonal) [34,35]. The peaks at 24.98° and 42.96° correspond to the (0 0 2) and (1 1 1) atomic planes, respectively [35]. Fig. 2(c) shows the Raman spectrum obtained for candle soot. Five Raman bands are observed at 1155, 1250, 1360, 1510, and 1611 cm^{-1}. The vibrational bands were found to be in good agreement with different hydrocarbons containing carbon chains. The most intense peak at 1611 cm^{-1} could be assigned to the E_{2g} stretching mode of the sp^2 C—C bond of amorphous graphitic hydrocarbon. The peak observed at 1360 cm^{-1} could be assigned to the A_{1g} symmetry because of the sp^3 bond present in distorted amorphous graphitic hydrocarbons. Weak bands appeared at 1155 and 1250 cm^{-1} as a result of the molecular carbon present in the soot. The band at 1510 cm^{-1} could be assigned to the stretching mode of distorted graphite [34]. Fig. 2(d) and (e) presents SEM micrographs of the uncoated and coated BCZTO samples, respectively. The SEM micrograph of the uncoated BCZTO depicts closely packed grains, which indicate its dense structure. No major porosity was observed on the surface of the sample. Uniformly distributed nanoparticles can be observed on the surface of the coated BCZTO, as shown in Fig. 2(e). Fig. 2(f) shows the cross section of the candle soot-coated BCZTO sample. The thickness of the candle soot coating was found to be approximately 20 µm over the surface. The structure actually showed a net-shaped porous structure formed by the agglomeration of nanoparticles. The surface area of the candle soot was found to be 60.848 m^2/g.

The surface potential values obtained for the BCZTO poled and unpoled samples (shown in the inset) are shown in Fig. 3. The highest surface potential obtained for the poled sample was ~1.5 V; whereas, the highest surface potential obtained for the unpoled sample was ~34 mV. These values indicate the effect of poling on the surface potential of the ferroelectric BCZTO sample.

To investigate the effect of ferroelectricity on the adsorption capacity of a candle soot-coated BCZTO sample, the absorption

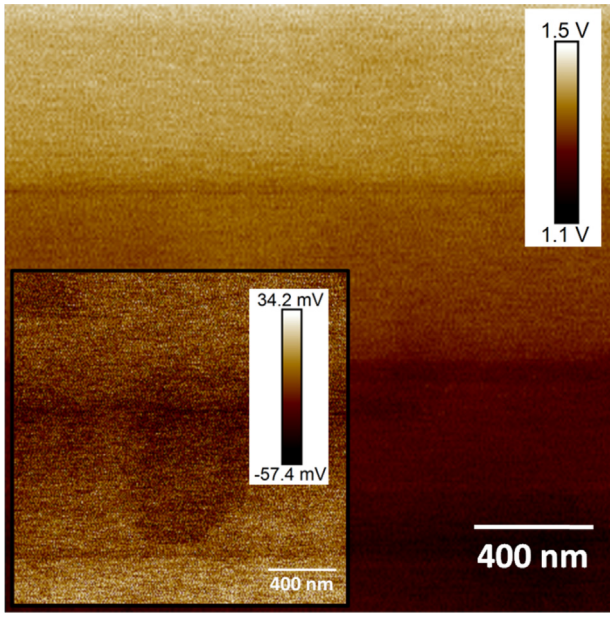

Fig. 3. Surface potential of poled and unpoled BCZTO samples (shown in inset for unpoled material).

capacity of the candle soot powder was first investigated. Then, the adsorption capacities of the candle soot-coated BCZTO (poled and unpoled) samples were investigated. The adsorption capacity of the candle soot was found to be highly dependent on the pH value of the dye solution. The effect of the pH value on the percentage of MB dye adsorbed on the candle soot powder is shown in Fig. 4. The candle soot was found to adsorb ~65%, 80%, and 90% of the MB dye in acidic, neutral, and basic media, respectively, within 3 h. This clearly indicated that an increase in the pH value led to an increase in the adsorbance of dye for the candle soot. The candle soot had a negative charge. In the acidic medium, this negative charge attracted H^+ ions (the major ions in the acidic medium), which were adsorbed on the candle soot surface. Because of this, the adsorption sites for dye molecules decreased. Hence, the adsorption of the MB dye decreased in the acidic medium. As the pH value increased, the adsorption of H^+ decreased. Hence, more adsorption

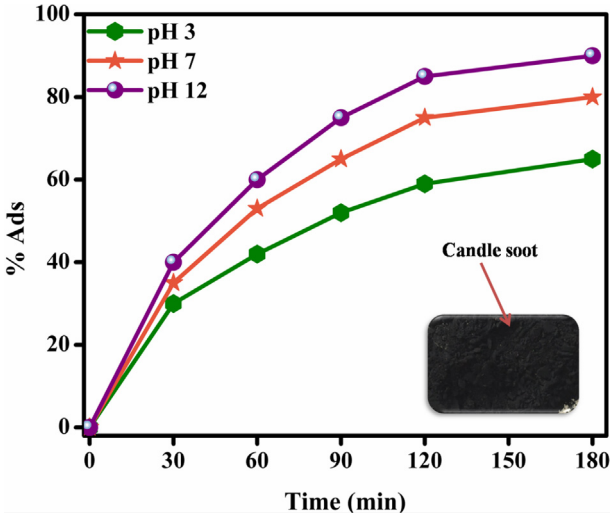

Fig. 4. Adsorption vs. time plots obtained for adsorption of MB dye using candle soot (powder) in acidic, neutral, and basic media.

sites were available for dye adsorption, and the adsorption of dye increased with an increase in the pH value of the medium. The maximum adsorption of MB dye was observed in the basic medium.

Fig. 5(a) and (b) show the $\frac{C}{C_0}$ vs. time plots for the adsorption of MB dye using uncoated BCZTO samples (both poled and unpoled) and candle soot-coated BCZTO samples (both unpoled and poled) at a pH = 7, where C represents the dye solution concentration at any time 't' and C_o represents the initial concentration of the dye solution. A decrease in the $\frac{C}{C_0}$ ratio is an indicator of an increase in the adsorbance of dye. No change in the $\frac{C}{C_0}$ values in the case of pure MB dye indicates its stable nature. Moreover, the value of $\frac{C}{C_0}$ changed from 1 to 0.96, 0.89, and 0.91 for the adsorption of dye using the uncoated-unpoled sample, positive poled surface of an uncoated sample, and negative poled surface of an uncoated sample, respectively. Hence, a very small adsorption of MB dye was observed using the uncoated unpoled and poled samples. The value of $\frac{C}{C_0}$ changed from 1 to 0.88, 0.67, and 0.70 for the adsorption of dye using the coated-unpoled sample, positive polarity of the poled surface of a coated sample, and negative polarity of the poled surface of a coated sample, respectively. This clearly shows that the adsorption values were increased by the use of a candle soot coating on the BCZTO samples compared with uncoated samples.

The increase in the adsorption value was mainly due to the significant adsorption capability of candle soot provided by its porous structure. Moreover, in the case of coated samples, poled samples were found to have more adsorption than unpoled samples for the same duration. This clearly shows that the ferroelectric surface charge had a positive effect on the adsorption of MB dye. To understand the effect of ferroelectric remnant polarisation on adsorption, the effect of the pH value was incorporated. Fig. 5(c) and (d) show $\frac{C}{C_0}$ vs. time plots for the adsorption of MB dye using coated BCZTO samples (both poled and unpoled) at pH values of 3 (acidic medium) and 12 (basic medium), respectively. In the acidic medium, the candle soot coated on the positive side showed the maximum adsorption of MB dye (the value of $\frac{C}{C_0}$ was changed from 1 to 0.16 within 3 h). The candle soot coated on the negative side showed significantly less adsorption than that on the positive side. The value of $\frac{C}{C_0}$ changed from 1 to 0.83 within 3 h for the negative side. In the basic medium, the results were reversed. The candle soot coated on the negative side showed the maximum adsorption (the value of $\frac{C}{C_0}$ changed from 1 to 0.08 within 3 h). The candle soot coated on the positive side showed significantly less adsorption than that on the negative side. The value of $\frac{C}{C_0}$ changed from 1 to 0.81 within 3 h for the negative side.

This could easily be explained by investigating the availability of adsorption sites while considering the ferroelectric charge and medium ion adsorption. Because the negative charge present on the candle soot was very small compared with the surface potential, the net charge on the candle soot-coated poled sample was the charge of the candle soot-coated poled surface. In the case of dye adsorption using candle soot coated on the positive surface of a poled BCZTO sample in an acidic medium, the candle soot became positively charged. Hence, it repelled the major H^+ ions present in the acidic medium and provided more adsorption sites for the MB dye. In the case of dye adsorption using candle soot coated on the negative surface of a poled BCZTO sample in an acidic medium, the major H^+ ions were adsorbed on the surface because of their attraction, and fewer adsorption sites were available for the MB dye. In the case of the basic medium, the adsorption sites were taken by OH^- ions (the major ions present in the basic medium) when candle soot was coated on the positive side.

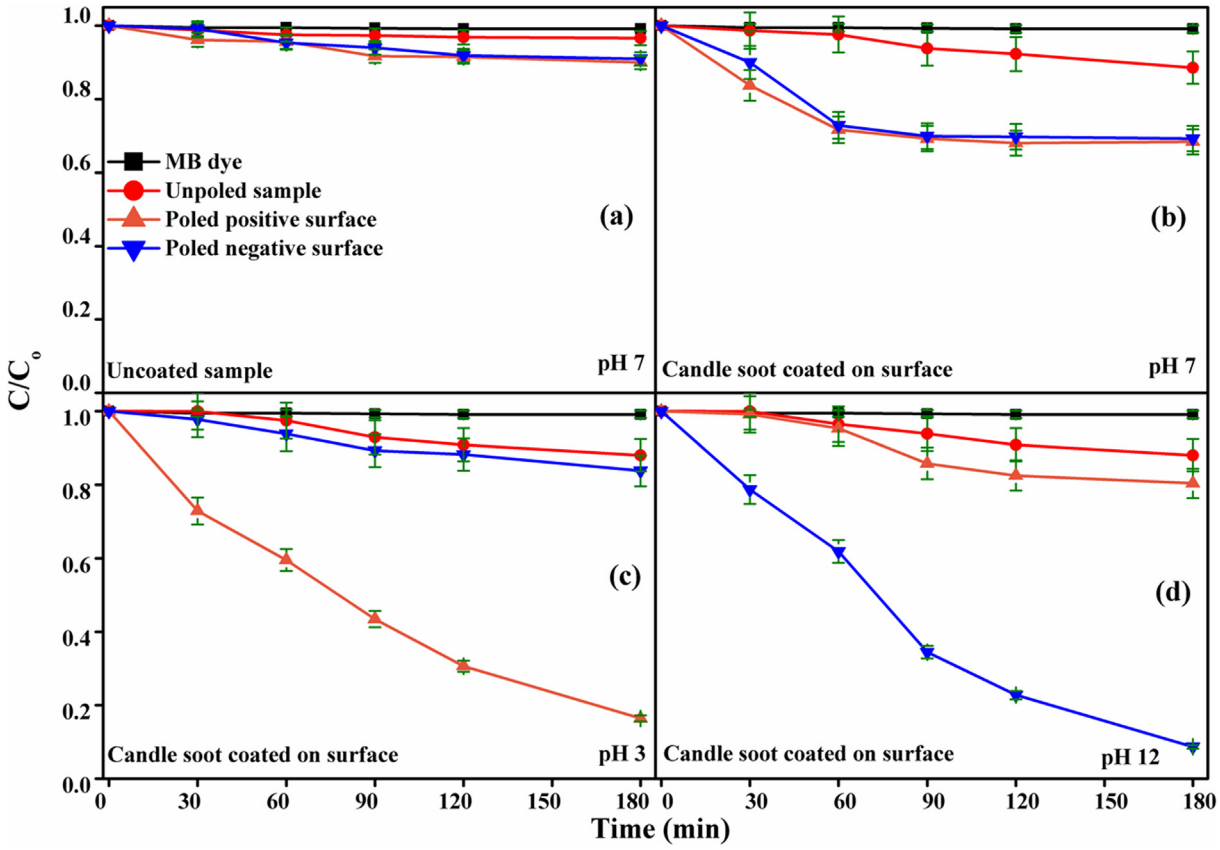

Fig. 5. $\frac{C}{C_0}$ vs. time plots for adsorption of MB dye using uncoated BCZTO samples (both poled and unpoled) and candle soot-coated BCZTO samples (both unpoled and poled) at pH = 3, 7, and 12.

The adsorption sites were available in the case where the candle soot was coated on the negative side because of the repulsion between the negative surface and OH^- ions. Hence, the candle soot coating on the positive surface in the case of an acidic medium and candle soot coating on the negative surface in the case of a basic medium provided promising adsorption properties. The adsorption property of the candle soot-coated poled BCZTO could be easily tuned by changing the surface potential and pH value of the solution.

In addition to the effect of ferroelectricity on the adsorption behaviour, it was very interesting to investigate the effect of ferroelectricity on the wettability of the candle soot coated on the BCZTO sample. The contact angle of the candle soot coated on an unpoled BCZTO sample was observed to be 140.4°. The contact angle of the candle soot coated on the unpoled BCZTO sample showed a negligible change (~2°) with an increase in temperature from 30 to 70 °C (the figure is not shown here). However, the candle soot coated on the poled BCZTO sample showed a significant change in the contact angle with an increase in temperature from 30 to 70 °C. Fig. 6 shows the contact angle vs. temperature plots obtained in the cases of candle soot coated on the positive surface of a poled sample and candle soot coated on the negative surface of a poled sample. In the case of candle soot coated on a positive surface, a decreasing trend for the contact angle (~148–134°) was found with an increase in temperature (30–70 °C). However, in the case of candle soot coated on a negative surface (~139–148°), an increasing trend for the contact angle was found with an increase in temperature. The change in the contact angle due to temperature was found in the case of poled samples, but this change was not observed in the case of the unpoled BCZTO sample. Hence, the change in the contact angle was not actually due to

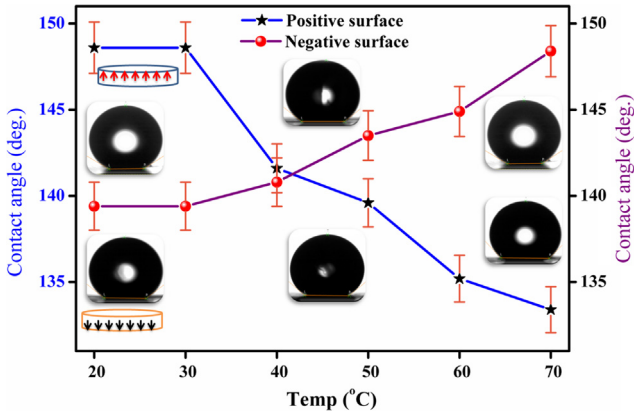

Fig. 6. Contact angle vs. temperature plots for candle soot coating on positive surface and candle soot coating on negative surface of poled BCZTO sample.

temperature. The change in the contact angle of the poled BCZTO was mainly due to changes in the poling magnitude and direction with a change in temperature.

To validate this argument, the reversibility of the change in the contact angle was demonstrated. Fig. 7 shows the reversible nature of the change in the contact angle in the cases of both candle soot coated on the positive surface of a poled sample and candle soot coated on the negative surface of a poled sample. It can easily be seen in Fig. 7 that any change in the contact angle achieved with a change in temperature could be reversed to the initial value of the contact angle when the temperature returned to its initial value. This indicates that, in the case of candle soot coated on a

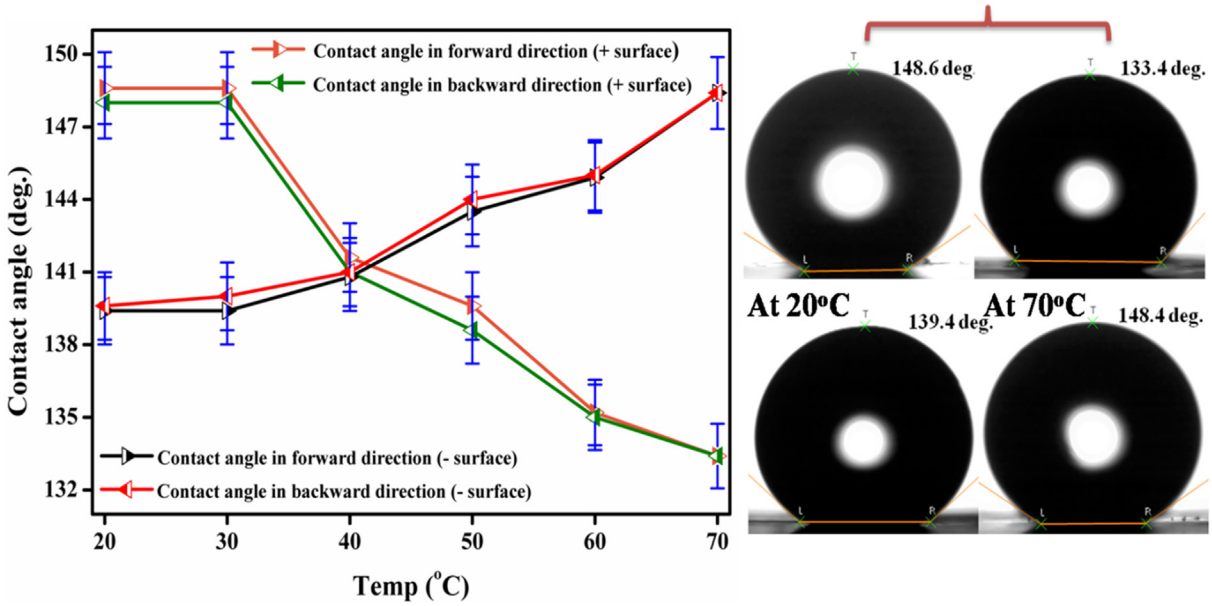

Fig. 7. (a) Variation of contact angle with change in temperature for candle soot coatings on positive and negative surfaces of poled BCZTO, and (b) contact angles at 20 °C and 70 °C for candle soot coatings on positive and negative surfaces of poled BCZTO sample.

positive surface, an increasing trend for the contact angle (~134–147.5°) was found with a decrease in temperature (70–30 °C). However, in the case of candle soot coated on a negative surface, a decreasing trend for the contact angle (~148–139°) was found with a decrease in temperature (70–30 °C).

This reversible change in the contact angle was mainly due to a change in the strength of the hydrogen bonding between the water molecules and candle soot. It is well reported in the literature that a change in the orientation of water molecules affects the formation of hydrogen bonding between water molecules and the surface of carbon soot, which affects the wettability behaviour of the surface [36–41]. The carbonyl functional group (C═O) present in candle soot forms hydrogen bonds with water molecules, with the strength of the bond depending upon the orientation of the water molecule [35]. The surface becomes hydrophobic when the orientation of the water near the surface become such that the O—H bond of the water is at an angle with the normal to the surface, which lessens the strength of the hydrogen bond and makes

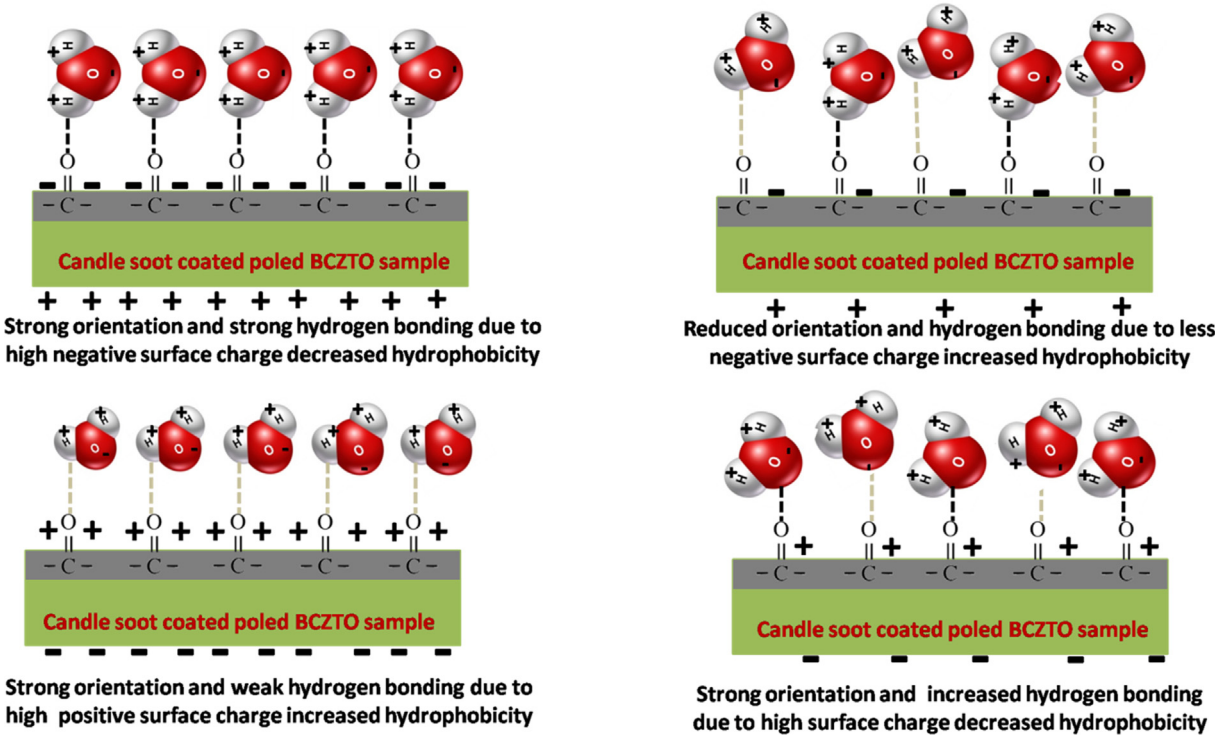

Fig. 8. Mechanism of change for contact angle with change in ferroelectric surface charge (dark dotted lines show strong hydrogen bonding and light dotted lines show weak hydrogen bonding).

the surface more hydrophobic [42]. Similarly, in the present case, the changes in hydrophobicity with changes in the temperature and ferroelectric charge could be explained in terms of the orientation of water molecules with respect to the ferroelectric charge. Water is a polar molecule (H—OH). Thus, the water molecules in a drop were oriented in accordance to the charge present on the surface. In the case of a candle soot coating on a negative surface, the negative charge acquired by the candle soot attracted the H and repelled the O of the water. In the case of a candle soot coating on the negative side at 30 °C, most of the water molecules came into contact with the surface in an oriented way (an O—H bond perpendicular to the surface), and this orientation favoured the hydrogen bond formation between the water molecules and surface. Thus, a lower contact angle was observed in this case. With an increase in temperature, the orientation of the dipoles present in the ferroelectric materials started to diminish, which decreased the negative charges present on the surface and candle soot. The lack of a negative charge caused the randomness of the water molecule orientation to increase. As a result, the strength of some of the hydrogen bonds decreased, and the contact angle increased.

In the case of the candle soot coating on the positive surface, the positive charge acquired by the candle soot (neglecting the negligible negative charge on the candle soot compared with the ferroelectric charge) attracted the O and repelled the H of the water as result of the presence of negative dipole charges on the O and positive dipole charges on the H. In the case of the candle soot coating on the positive side at 30 °C, most of the water molecules came into contact with the surface in an oriented way. However, this orientation reduced the hydrogen bond strength between the water molecules and surface (the O—H bond was at an angle with the normal to surface). Thus, a very high contact angle was observed in this case. With an increase in temperature, the orientation of the dipoles present in the ferroelectric materials started to diminish, which decreased the positive charge present on the surface and candle soot. Because of the lack of a positive charge, the randomness of the water molecule orientation also increased. With this increase in randomness, the strength of some hydrogen bonds increased, which caused the contact angle to increase. Fig. 8 shows a schematic of the mechanism behind the change in the contact angle with a change in temperature in the case of the BCZTO poled sample.

The reversible change in the contact angle actually makes it possible to tune the contact angle according to the application. For example, in the case of dye adsorption, it is important to increase the contact time between the dye and coating, which is possible by taking advantage of smaller contact angles. However, in the case of self-cleaning applications, hydrophobicity is required, which can be achieved by increasing the contact angle.

Conclusions

A candle soot coating on a ferroelectric BCZTO sample was found to be a promising candidate for the adsorption of the MB dye pollutant. Enhanced adsorption could be achieved using a poled ferroelectric BCZTO sample. The candle soot coating on the positive surface in the case of an acidic medium and the candle soot on the negative surface in the case of a basic medium provided high MB dye adsorption values. The wettability characteristics of the candle soot-coated poled BCZTO sample could be easily tuned according to the application by varying the poling charge.

Conflict of interest

The authors have declared no conflict of interest.

Compliance with Ethics Requirements

This article does not contain any studies with human or animal subjects.

Acknowledgements

RV thanks SERB, India for financial support under the project SERB/F/6647/2015-2016. (YSS/2014/000925).

References

[1] Ahmed B, Ojha AK, Singh A, Hirsch F, Fischer I, Patrice D, et al. Well-controlled in-situ growth of 2D WO_3 rectangular sheets on reduced graphene oxide with strong photocatalytic and antibacterial properties. J Hazard Mater 2018;347:266–78.
[2] Dwivedi AK. Researches in water pollution: a review. Int Res J Nat Appl Sci 2017;4(1):118–42.
[3] Holkar CR, Jadhav AJ, Pinjari DV, Mahamuni NM, Pandit AB. A critical review on textile wastewater treatments: possible approaches. J Environ Manage 2016;182(142):351–66.
[4] Bharathi KS, Ramesh ST. Removal of dyes using agricultural waste as low-cost adsorbents: a review. Appl Water Sci 2013;3(4):773–90.
[5] Iqbal MJ, Ashiq MN. Adsorption of dyes from aqueous solutions on activated charcoal. J Hazard Mater 2007;139(1):57–66.
[6] Al-Qodah Z. Adsorption of dyes using shale oil ash. Water Res 2000;34 (17):4295–303.
[7] Bhatnagar A, Jain AK. A comparative adsorption study with different industrial wastes as adsorbents for the removal of cationic dyes from water. J Colloid Interface Sci 2005;281(1):49–55.
[8] Yagub MT, Sen TK, Afroze S, Ang HM. Dye and its removal from aqueous solution by adsorption: a review. Adv Colloid Interface Sci 2014;209:172–84.
[9] Byrne C, Subramanian G, Pillai SC. Recent advances in photocatalysis for environmental applications. J Environ Chem Eng 2018;6(3):3531–55.
[10] Xie X, Mao C, Liu X, Zhang Y, Cui Z, Yang X, et al. Synergistic bacteria killing through photodynamic and physical actions of graphene oxide/Ag/Collagen coating. ACS Appl Mater Interfaces 2017;9(31):26417–28.
[11] Tan L, Li J, Liu X, Cui Z, Yang X, Zhu S, et al. Rapid biofilm eradication on bone implants using red phosphorus and near-infrared light. Adv Mater 2018;30 (31):1801808.
[12] Feng Z, Liu X, Tan L, Cui Z, Yang X, Li Z, et al. Electrophoretic deposited stable chitosan@MoS_2 coating with rapid in situ bacteria-killing ability under dual-light irradiation. Small 2018;14(21):1704347.
[13] Tan L, Li J, Liu X, Cui Z, Yang X, Yeung KWK, et al. In situ disinfection through photoinspired radical oxygen species storage and thermal-triggered release from black phosphorous with strengthened chemical stability. Small 2018;14 (9):1703197.
[14] Gupta VK, Gupta B, Rastogi A, Agarwal S, Nayak A. A comparative investigation on adsorption performances of mesoporous activated carbon prepared from waste rubber tire and activated carbon for a hazardous azo dye-Acid Blue 113. J Hazard Mater 2011;186(1):891–901.
[15] Singh VP, Vaish R. Adsorption of dyes onto candle soot: equilibrium, kinetics and thermodynamics. Eur Phys J Plus 2018;133(10):446.
[16] Seo K, Kim M, Kim DH. Candle-based process for creating a stable superhydrophobic surface. Carbon NY 2014;68:583–96.
[17] Li J, Yan L, Tang X, Feng H, Hu D, Zha F. Robust superhydrophobic fabric bag filled with polyurethane sponges used for vacuum-assisted continuous and ultrafast absorption and collection of oils from water. Adv Mater Interfaces 2016;3(9):1500770.
[18] Li J, Jing Z, Zha F, Yang Y, Wang Q, Lei Z. Facile spray-coating process for the fabrication of tunable adhesive superhydrophobic surfaces with heterogeneous chemical compositions used for selective transportation of microdroplets with different volumes. ACS Appl Mater Interfaces 2014;6 (11):8868–77.
[19] Li J, Kang R, Tang X, She H, Yang Y, Zha F. Superhydrophobic meshes that can repel hot water and strong corrosive liquids used for efficient gravity-driven oil/water separation. Nanoscale 2016;8(14):7638–45.
[20] Ania CO, Béguin F. Mechanism of adsorption and electrosorption of bentazone on activated carbon cloth in aqueous solutions. Water Res 2007;41 (15):3372–80.
[21] Ma CY, Huang SC, Chou PH, Den W, Hou CH. Application of a multiwalled carbon nanotube-chitosan composite as an electrode in the electrosorption process for water purification. Chemosphere 2016;146:113–20.
[22] Wang J, Neaton JB, Zheng H, Nagarajan V, Ogale SB, Liu B, et al. Epitaxial $BiFeO_3$ multiferroic thin film heterostructures. Science 2003;299(5613):1719–22.
[23] Whatmore RW, Osbond PC, Shorrocks NM. Ferroelectric materials for thermal IR detectors. Ferroelectrics 1987;76(1):351–67.
[24] Myers LE, Eckardt RC, Fejer MM, Byer RL, Bosenberg WR, Pierce JW. Quasi-phase-matched optical parametric oscillators in bulk periodically poled $LiNbO_3$. J Opt Soc Am B 1995;12(11):2102.

[25] Tombak A, Maria JP, Ayguavives FT, Jin Z, Stauf GT, Kingon AI, et al. Voltage-controlled RF filters employing thin-film barium-strontium-titanate tunable capacitors. IEEE Trans Microw Theory Tech 2003;51(2I):462–7.
[26] Lanfredi S, Palacio G, Bellucci FS, Colin CV, Nobre MAL. Thermistor behaviour and electric conduction analysis of Ni-doped niobate ferroelectric: the role of multiple β parameters. J Phys D Appl Phys 2012;45(43).
[27] Huang J, Yuan Y, Shao Y, Yan Y. Understanding the physical properties of hybrid perovskites for photovoltaic applications. Nat Rev Mater 2017;2 (7):17042.
[28] Li J, Zhang G, Han S, Cao J, Duan L, Zeng T. Enhanced solar absorption, visible-light photocatalytic and photoelectrochemical properties of aluminium-reduced $BaTiO_3$ nanoparticles. Chem Commun 2017;54(7):723–6.
[29] Lin X, Xing J, Wang W, Shan Z, Xu F, Huang F. Photocatalytic activities of heterojunction semiconductors Bi_2O_3/$BaTiO_3$: a strategy for the design of efficient combined photocatalysts. J Phys Chem C 2007;111(49):18288–93.
[30] Tsai WT, Hsu HC, Su TY, Lin KY, Lin CM. Removal of basic dye (methylene blue) from wastewaters utilizing beer brewery waste. J Hazard Mater 2008;154(1–3):73–8.
[31] Tan IAW, Ahmad AL, Hameed BH. Adsorption of basic dye using activated carbon prepared from oil palm shell: batch and fixed bed studies. Desalination 2008;225(1–3):13–28.
[32] Patel S, Chauhan A, Electrocaloric Vaish R. Behavior and temperature-dependent scaling of dynamic hysteresis of $Ba_{0.85}Ca_{0.15}Ti_{0.9}Zr_{0.1}O_3$ ceramics. Int J Appl Ceram Technol 2015;12(4):899–907.
[33] Sharma M, Singh VP, Singh S, Azad P, Ilahi B, Madhar NA. Porous $Ba_{0.85}Ca_{0.15}Zr_{0.1}Ti_{0.9}O_3$ ceramics for pyroelectric applications. J Electron Mater 2018;47(8):4882–91.
[34] Sharma M, Kumar A, Singh VP, Kumar R, Vaish R. Large gain in pyroelectric energy conversion through a candle soot coating. Energy Technol 2018;6 (5):950–5.
[35] Sahoo BN, Kandasubramanian B. An experimental design for the investigation of water repellent property of candle soot particles. Mater Chem Phys 2014;148(1–2):134–42.
[36] Azimi G, Dhiman R, Kwon HM, Paxson AT, Varanasi KK. Hydrophobicity of rare-earth oxide ceramics. Nat Mater 2013;12(4):315–20.
[37] Jensen MØ, Mouritsen OG, Peters GH. The hydrophobic effect: molecular dynamics simulations of water confined between extended hydrophobic and hydrophilic surfaces. J Chem Phys 2004;120(20):9729–44.
[38] Giovambattista N, Rossky PJ, Debenedetti PG. Effect of temperature on the structure and phase behavior of water confined by hydrophobic, hydrophilic, and heterogeneous surfaces. J Phys Chem B 2009;113(42):13723–34.
[39] Remsing RC, Weeks JD. Hydrophobicity scaling of aqueous interfaces by an electrostatic mapping. J Phys Chem B 2015;119(29):9268–77.
[40] Ren H, Zhang L, Li X, Li Y, Wu W, Li H. Interfacial structure and wetting properties of water droplets on graphene under a static electric field. Phys Chem Chem Phys 2015;17(36):23460–7.
[41] Strazdaite S, Versluis J, Bakker HJ. Water orientation at hydrophobic interfaces. J Chem Phys 2015;143(8):084708.
[42] Giovambattista N, Debenedetti PG, Rossky PJ. Effect of surface polarity on water contact angle and interfacial hydration structure. J Phys Chem B 2007;111(32):9581–7.